

Electronic supporting information for

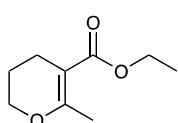
“Investigating the origin of entropy-derived rate accelerations in ionic liquids”

Hon Man Yau,^{a,b} Anna K. Croft^b and Jason B. Harper^{a,*}

^aSchool of Chemistry, University of New South Wales, Sydney, NSW, 2052, Australia

^bSchool of Chemistry, University of Wales Bangor, Bangor, Gwynedd LL57 2UW, United Kingdom

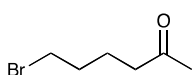
Synthesis of 6-methyl-2,3,4,5-tetrahydropyridine (7)



Ethyl 6-methyl-3,4-dihydro-2H-pyran-5-carboxylate. The pyran was synthesised according to a literature procedure.¹ To a solution of 1,3-dibromopropane (2.01 g, 9.96 mmol) and ethyl acetoacetate (2.65 g, 20.4 mmol, 2 equiv.) in dry acetone (15 mL), potassium carbonate (4.02 g, 29.1 mmol, 3 equiv.)

was added and the mixture was heated under reflux for *ca.* 72 hours. The mixture was allowed to cool to room temperature, after which excess potassium carbonate and the potassium bromide by-product were removed by filtration and the filtrate collected. Acetone was removed under reduced pressure (*ca.* 210 mmHg) to yield a light yellow oil consisting of unreacted ethyl acetoacetate and the pyran product. The mixture was separated using silica gel chromatography (hexane:ethyl acetate) to give the final product as a colourless liquid (0.52 g, 3.06 mmol, 31%). ¹H NMR (CDCl₃, 500 MHz) δ_{ppm} 1.27 (t, $J_3 = 7.1$ Hz, 3H, OCH₂CH₃), 1.82 (tt, $J_{3(\text{H}2)} = 5.3$ Hz, $J_{3(\text{H}4)} = 6.5$ Hz, 2H, CH₂CH₂C_q), 2.21 (s, 3H, C_qCH₃), 2.30 (t, $J_3 = 6.5$ Hz, 2H, CH₂C_q), 4.00 (t, $J_3 = 5.3$ Hz, 2H, CH₂CH₂O), 4.15 (q, $J_3 = 7.1$ Hz, 2H, OCH₂CH₃);* ¹³C{¹H} NMR (CDCl₃, 125 MHz) δ_{ppm} 14.6 (OCH₂CH₃), 20.4 (C_qCH₃), 21.5 and 21.8 (CH₂CH₂C_q), 66.8 (CH₂CH₂O), 101.5 (CH₂CH₂C_q), 165.0 (CH₃C_q), 168.9 (C=O).

It should be noted that, in order to maximise yield, purification using column chromatography was not carried out in subsequent syntheses of 6-bromohexan-2-one as the conditions used in the hydrolysis of the pyran also facilitates decomposition of ethyl acetoacetate into methanol, acetone and carbon dioxide.



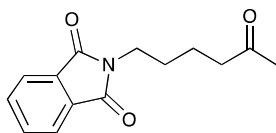
6-Bromohexan-2-one. A modified literature procedure³ was used to synthesise the hexanone, where aqueous hydrobromic acid (48% w/v, 60 mL, 1.10 mol) was added with stirring to a solution containing ethyl 6-methyl-3,4-dihydro-2H-pyran-

5-carboxylate and ethyl acetoacetate, obtained from 1,3-dibromopropane (20.0 g, 99.1 mmol) and ethyl acetoacetate (27.0 g, 208 mmol, 2 equiv.) and potassium carbonate (41.0 g, 297 mmol, 3 equiv.) using the procedure stated above. Formation of carbon dioxide was observed immediately corresponding to the decarboxylation of the pyran and the orange solution was then heated to reflux for *ca.* 36 hours after effervescence has subsided.

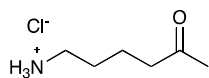
The reaction was allowed to cool to room temperature and poured onto ice (*ca.* 200 g) to give a crude, dark brown, product as a separate layer. The crude product was separated, diluted with chloroform (25 mL) and washed with saturated sodium bicarbonate (3 x 15 mL) followed by deionised water (20 mL). The organic layer was dried over magnesium sulphate and the solvent

* Higher order coupling was observed in all protons on the pyran except for those on the ethyl carboxylate tether. It is not uncommon for such higher order structures to be observed in the ¹H NMR spectrum of a pyran.²

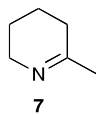
removed under reduced pressure (*ca.* 210 mmHg) to give the product as a dark brown liquid (13.5 g, 75.5 mmol, 76%) and used without further purification. ^1H NMR (CDCl_3 , 500 MHz) δ_{ppm} 1.66-1.92 (m, 4H, $\text{CH}_2\text{BrCH}_2\text{CH}_2$), 2.14 (s, 3H, CH_3), 2.47 (t, $J_3 = 7.1$ Hz, 2H, $\text{CH}_2\text{C}=\text{O}$), 3.40 (t, $J_3 = 6.7$ Hz, 2H, CH_2Br); $^{13}\text{C}\{^1\text{H}\}$ NMR (CDCl_3 , 125 MHz) δ_{ppm} 22.3 ($\text{CH}_2\text{BrCH}_2\text{CH}_2$), 29.9 (CH_2BrCH_2), 32.0 (CH_3), 33.2 (CH_2Br), 42.5 ($\text{CH}_2\text{C}=\text{O}$), 208.2 ($\text{C}=\text{O}$).



***N*-(6-Oxohexyl)phthalimide:** Potassium phthalimide (18.91 g, 102 mmol) was added to a solution of 6-bromohexan-2-one (13.5 g, 75.5 mmol) in *N,N*-dimethylformamide (DMF) (50 mL).⁴ After heating at 65°C with stirring for *ca.* 4 hours, the mixture was poured into deionised water (250 mL) and the product extracted using chloroform (3 x 40 mL)[†]. The combined organic extract, after having its volume reduced under reduced pressure (*ca.* 210 mmHg), was washed with aqueous sodium hydroxide (40% w/v, 3 x 20 mL) then deionised water (2 x 25 mL) and dried over magnesium sulphate. Chloroform was removed under reduced pressure (*ca.* 210 mmHg) and traces of DMF at further reduced pressure (< 5 mmHg, 50°C) to give the product as an orange solid (14.94 g, 60.91 mmol, 81%) and used in subsequent syntheses without further purification. ^1H NMR (CDCl_3 , 500 MHz) δ_{ppm} 1.54-1.76 (m, 4H, $\text{CH}_2\text{CH}_2\text{CH}_2\text{C}=\text{O}$), 2.13 (s, 3H, CH_3), 2.49 (t, $J_3 = 7.1$ Hz, 2H, $\text{CH}_2\text{C}=\text{O}$), 3.69 (t, $J_3 = 6.7$ Hz, 2H, NCH_2), 7.71 and 7.83 (m, 4H, Ar-H); $^{13}\text{C}\{^1\text{H}\}$ NMR (CDCl_3 , 125 MHz) δ_{ppm} 21.1 ($\text{CH}_2\text{CH}_2\text{C}=\text{O}$), 28.3 (NCH_2CH_2), 30.3 (CH_3), 37.8 (NCH_2), 43.2 ($\text{CH}_2\text{C}=\text{O}$), 123.6, 132.4 and 134.3 (Ar-C), 168.7 ($\text{NC}=\text{O}$), 208.7 ($\text{CH}_3\text{C}=\text{O}$).



6-Aminohexane-2-one hydrochloride: *N*-(6-Oxohexyl)phthalimide (3.19 g, 13.0 mmol) was mixed with aqueous hydrochloride acid (32% w/v, 20 mL, 630 mmol) and heated under reflux with stirring for *ca.* 80 hours.⁴ The mixture was allowed to cool and the phthalic acid precipitate was removed by filtration to give a dark orange solution. The aqueous layer was washed with diethyl ether (2 x 15 mL) followed by removal of water under reduced pressure to give the crude product as an orange solid (1.48 g, 10.8 mmol, 83%), which was used without further purification. ^1H NMR (D_2O , 400 MHz) δ_{ppm} 1.51-1.71 (m, 4H, $\text{NCH}_2\text{CH}_2\text{CH}_2$), 2.15 (s, 3H, CH_3),[‡] 2.56 (t, $J_3 = 6.2$ Hz, 2H, $\text{C}_\alpha\text{CH}_2$),[§] 3.39 (m, 2H, NCH_2); $^{13}\text{C}\{^1\text{H}\}$ NMR (H_2O , 100 MHz) δ_{ppm} 17.0 ($\text{CH}_2\text{CH}_2\text{C}=\text{O}$), 29.9 (NCH_2CH_2), 32.0 (CH_3), 33.2 (NCH_2), 42.5 ($\text{CH}_2\text{C}=\text{O}$), 208.2 ($\text{C}=\text{O}$). ^1H NMR signals were demonstrated to be concentration-dependent but the relative positions of the resonances do not change.



6-Methyl-2,3,4,5-tetrahydropyridine (7): Aqueous sodium hydroxide (40% w/v, 10 mL, 40 mmol) was added dropwise to a solution of 6-aminohexane-2-one hydrochloride (1.48 g, 9.76 mmol) in deionised water (10 mL) cooled using an ice bath to give an orange organic layer that is the crude product.⁴ The organic layer was separated from the bulk and a further extraction of the aqueous layer was carried out using diethyl ether (2 x 15 mL). The combined organic layers were dried with solid sodium hydroxide and diethyl ether was removed under reduced to give an oil dark orange in colour. Although the product could be distilled under reduced pressure (b.p. 87-90 °C, 210 mmHg), the distillate obtained in this fashion was slight yellow and small amounts of impurities were observed in the ^1H NMR spectrum; these impurities are possibly the result of thermal decomposition during distillation. Consequently, purification was

[†] An emulsion may form at this stage, resulting in difficulties in separation. Separation may be assisted by additional deionised water and/or chloroform.

[‡] Higher order coupling was also observed for this signal.

[§] Higher order coupling was also observed for this signal.

achieved by fractional distillation, collecting the product using a liquid nitrogen trap at further reduced pressure (< 5 mmHg) to give the product as a colourless liquid (0.64 g, 6.57 mmol, 67%). ^1H NMR (CDCl_3 , 500 MHz) δ_{ppm} 1.44-1.74 (m, 4H, $\text{NCH}_2\text{CH}_2\text{CH}_2$), 1.89 (s, 3H, CH_3), ** 2.11 (t, $J_3 = 6.7$ Hz, 2H, C_qCH_2), †† 3.51 (m, 2H, NCH_2); ‡‡ $^{13}\text{C}\{^1\text{H}\}$ NMR (CDCl_3 , 125 MHz) δ_{ppm} 19.7 ($\text{NCH}_2\text{CH}_2\text{CH}_2$), 21.8 (NCH_2CH_2), 27.6 (CH_3), 30.4 (C_qCH_2), 49.3 (NCH_2), 168.3 (C_q).

General procedures for kinetics experiments

Initially, a solution of the nucleophile of interest at the desired concentration (*ca.* 0.25 mol·L⁻¹ for where 6-methyl-2,3,4,5-tetrahydropyridine **7** was the nucleophile and *ca.* 0.50 mol·L⁻¹ for all other cases) was prepared by adding either dry acetonitrile (20% *d*₃ v/v) or dry [bmim][N(SO₂CF₃)₂] to a volumetric flask containing the appropriate amount of the nucleophile.

Each kinetic experiment was prepared by adding the solution prepared as described above (500 μL) to an NMR tube containing either benzyl bromide or *n*-bromobutane (10 mol% relative to the nucleophile). For the reaction between 6-methyl-2,3,4,5-tetrahydropyridine **7** and benzyl bromide **1d** in the ionic liquid, each sample was prepared in an ice bath to limit the extent of reaction prior to kinetic analysis. Note that for reactions where the ionic liquid was the solvent, a sealed capillary containing acetonitrile-*d*₃ was introduced into the NMR tube to allow the sample to be locked during kinetic analysis.

All reactions were monitored in an NMR machine at the desired temperatures as the reactions progressed, except for those between 2-methylpyridine **5** and *n*-bromobutane **4** due to the relatively slow reactions. In the latter cases a water bath was used instead and NMR spectra were periodically taken at *ca.* 283 K. The temperatures inside the bore of an NMR machine and the water bath were measured prior to each kinetic experiment using the same thermometer using a thermocouple fitted inside a 5 mm NMR tube containing either ethanol or ethylene glycol.

For the reaction between benzyl bromide and either 2-methylpyridine **5** or 6-methyl-2,3,4,5-tetrahydropyridine **7**, the reaction was monitored by following the signal corresponding to the protons on the halide-bearing carbon of the electrophile. For the reaction between *n*-bromobutane **4** and 2-methylpyridine **5**, the extent of reaction was deduced from the ratio of the starting material and the product using the signals corresponding to the substituted carbon belonging to the butyl backbone; sufficient relaxation delays were utilised to ensure validity in the relative integrations.

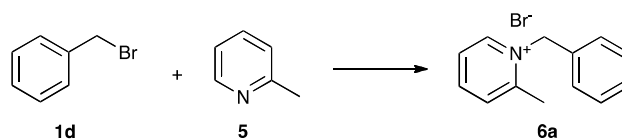
Finally, for the reaction between 6-methyl-2,3,4,5-tetrahydropyridine **7** and *n*-bromobutane **4**, a magnetic field intensity of 16.4 T (700 MHz) was necessary to obtain resolution for the proton signals belonging to the halide-bearing carbon on *n*-bromobutane in acetonitrile. In the case of the ionic liquid, quantitative ^1H - ^{13}C heteronuclear single quantum correlation (HSQC) spectroscopy was used to follow the proton-carbon cross coupling of the halide-bearing carbon of *n*-bromobutane **4** instead; it was not possible to follow the reaction using ^1H NMR spectroscopy due to significant overlap of the proton signals corresponding to the halide-bearing carbon and the α protons of 6-methyl-2,3,4,5-tetrahydropyridine **7**.

** Higher order coupling was observed.

†† Higher order coupling was observed.

‡‡ Higher order coupling was observed.

Activation parameters and the associated temperature-dependent rate constants for the reaction between benzyl bromide (1d) and 2-methylpyridine (5)



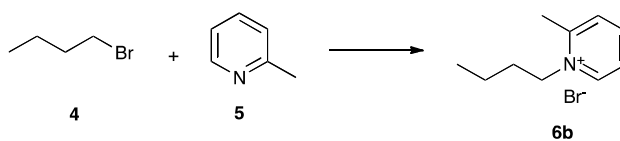
	$\Delta H^\ddagger / \text{J}\cdot\text{K}^{-1}\cdot\text{mol}^{-1}$	$\Delta S^\ddagger / \text{J}\cdot\text{K}^{-1}\cdot\text{mol}^{-1}$
Acetonitrile	48.1 ± 1.0	-223 ± 3
[bmim][N(SO ₂ CF ₃) ₂]	55.6 ± 0.6	-191 ± 2
Difference	7.3 ± 1.2	32 ± 4

§§[Nuc]_{CH₃CN}: 0.4974 mol·L⁻¹; [Nuc]_{IL}: 0.4976 mol·L⁻¹

Temperature / K	$k_{\text{obs}} / 10^{-5} \text{ mol}^{-1}\cdot\text{s}^{-1}$ (Acetonitrile)	$k_{\text{obs}} / 10^{-5} \text{ mol}^{-1}\cdot\text{s}^{-1}$ ([bmim][N(SO ₂ CF ₃) ₂])
278.1	-	2.67
278.1	-	2.77
278.1	-	2.86
289.6	-	7.60
289.6	3.24	7.75
289.6	3.39	8.03
289.6	3.51	8.09
300.7	-	19.2
300.7	7.17	19.6
300.7	7.25	19.7
300.7	7.50	19.9
311.5	15.7	-
311.5	15.8	-
311.5	16.4	-

§§ [Nuc] refers to the concentration of the nucleophile involved.

Activation parameters and the associated temperature-dependent rate constants for the reaction between *n*-bromobutane (4) and 2-methylpyridine (5)

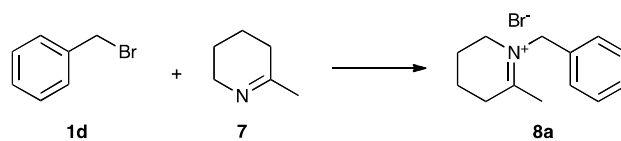


	$\Delta H^\ddagger / \text{J}\cdot\text{K}^{-1}\cdot\text{mol}^{-1}$	$\Delta S^\ddagger / \text{J}\cdot\text{K}^{-1}\cdot\text{mol}^{-1}$
Acetonitrile	64.7 ± 0.2	-220 ± 1
[bmim][N(SO ₂ CF ₃) ₂]	71.4 ± 0.2	-192 ± 1
Difference	6.0	26

[Nuc]_{CH₃CN}: 0.4974 mol·L⁻¹; [Nuc]_{IL}: 0.5004 mol·L⁻¹

Temperature / K	$k_{\text{obs}} / 10^{-7} \text{ mol}^{-1}\cdot\text{s}^{-1}$ (Acetonitrile)	$k_{\text{obs}} / 10^{-7} \text{ mol}^{-1}\cdot\text{s}^{-1}$ ([bmim][N(SO ₂ CF ₃) ₂])
315.0	-	11.0
315.0	4.89	11.1
315.0	4.91	11.2
315.0	4.93	11.2
315.0	4.97	11.2
324.8	-	26.4
324.8	10.8	26.6
324.8	10.9	26.7
324.8	11.0	26.9
324.8	11.0	27.1
334.9	24.0	63.4
334.9	24.1	63.4
334.9	24.1	63.7
334.9	24.2	63.7
334.9	24.4	64.3

Activation parameters and the associated temperature-dependent rate constants for the reaction between benzyl bromide (1d) and 6-methyl-2,3,4,5-tetrahydropyridine (7)

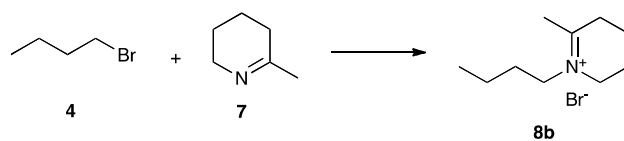


	$\Delta H^\ddagger / \text{J} \cdot \text{K}^{-1} \cdot \text{mol}^{-1}$	$\Delta S^\ddagger / \text{J} \cdot \text{K}^{-1} \cdot \text{mol}^{-1}$
Acetonitrile	43.6 ± 1.2	-211 ± 4
[bmim][N(SO ₂ CF ₃) ₂]	48.0 ± 1.1	-189 ± 4
Difference	4.4 ± 1.6	23 ± 6

[Nuc]_{CH₃CN}: 0.2500 mol·L⁻¹; [Nuc]_{IL}: 0.2476 mol·L⁻¹

Temperature / K	$k_{\text{obs}} / 10^{-4} \text{ mol}^{-1} \cdot \text{s}^{-1}$ (Acetonitrile)	$k_{\text{obs}} / 10^{-4} \text{ mol}^{-1} \cdot \text{s}^{-1}$ ([bmim][N(SO ₂ CF ₃) ₂])
268.1	-	1.81
268.1	-	2.00
268.1	-	2.05
278.1	-	4.24
278.1	1.77	4.36
278.1	2.01	4.45
278.1	2.11	4.49
288.1	-	9.99
288.1	-	10.1
288.1	-	10.1
289.6	4.23	
289.6	4.27	
289.6	4.36	
289.6	4.37	
300.7	9.08	
300.7	9.47	
300.7	9.48	
300.7	9.61	

Activation parameters and the associated temperature-dependent rate constants for the reaction between *n*-bromobutane (4) and 6-methyl-2,3,4,5-tetrahydropyridine (7)



	$\Delta H^\ddagger / \text{J} \cdot \text{K}^{-1} \cdot \text{mol}^{-1}$	$\Delta S^\ddagger / \text{J} \cdot \text{K}^{-1} \cdot \text{mol}^{-1}$
Acetonitrile	58.5 ± 8.9	-206 ± 27
[bmim][N(SO ₂ CF ₃) ₂]	85.0 ± 5.7	-112 ± 18
Difference	4.4 ± 1.6	94 ± 33

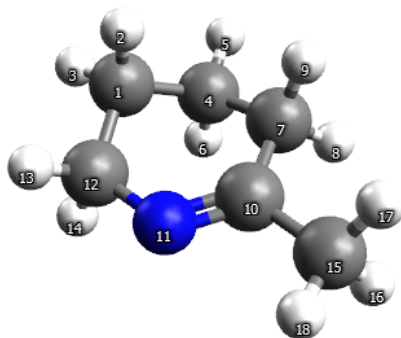
[Nuc]_{CH₃CN}: 0.2478 mol·L⁻¹; [Nuc]_{IL}: 0.2351 mol·L⁻¹

Temperature / K	$k_{\text{obs}} / 10^{-4} \text{ mol}^{-1} \cdot \text{s}^{-1}$ (Acetonitrile)	$k_{\text{obs}} / 10^{-4} \text{ mol}^{-1} \cdot \text{s}^{-1}$ ([bmim][N(SO ₂ CF ₃) ₂])
305.0	-	1.24
305.0	-	1.24
305.0	-	1.61
315.0	1.06	4.82
315.0	1.35	5.67
315.0	1.86	5.72
325.0	3.37	11.4
325.0	3.97	12.0
325.0	3.99	12.7
325.0	4.41	-
335.0	5.59	-
335.0	4.94	-
335.0	7.43	-

Computational Methods

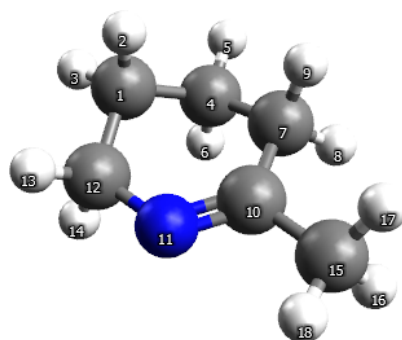
Molecular structures were calculated using Gaussian 03⁵ with the B3LYP/6-31G(d) method and RESP charges calculated for these structures using GAMESS⁶ at MP2/6-311+G(d,p)//B3LYP/6-31G(d). Molecular dynamics simulations were carried out using DL_POLY 2.20.⁷ Input configurations were generated using Aten,⁸ applying the Canongia Lopes forcefield⁹ for ionic liquid components and the OPLS-AA forcefield¹⁰⁻¹⁴ for other atoms. Structures of the nucleophiles were modelled as rigid bodies. All configurations were constructed as cubic boxes to give systems of low density, and these were then allowed to relax through a series of low-temperature, constant-pressure simulations, beginning with a timestep of 2×10^{-5} fs, to afford cells of the appropriate densities. Short and long-range cutoffs were set to 12.0 Å with an Ewald precision of 10^{-6} and preliminary runs of 400 ps at 400 K were used to equilibrate the system prior to the production runs. Data was collected for 4 ns trajectories at 400 K with a timestep of 2 fs with configurations saved at every 250 steps (0.5 ps).

Electrostatic potential charges for 2,3,4,5-tetrahydro-6-methylpyridine (7)



Label	Atom	Charge
1	C	-0.1544
2	H	0.0574
3	H	0.0151
4	C	0.0969
5	H	0.0066
6	H	0.0021
7	C	-0.1884
8	H	0.0479
9	H	0.0610
10	C	0.7218
11	N	-0.8734
12	C	0.3294
13	H	-0.0003
14	H	0.0120
15	C	-0.5654
16	H	0.1502
17	H	0.1458
18	H	0.1356

Cartesian coordinates used for 2,3,4,5-tetrahydro-6-methylpyridine (7) in molecular dynamics simulations



Label	Atom	x	y	z
1	C	-1.825	-0.057	0.344
2	H	-1.765	0.028	1.438
3	H	-2.888	-0.151	0.090
4	C	-1.207	1.189	-0.297
5	H	-1.731	2.101	0.011
6	H	-1.301	1.121	-1.389
7	C	0.276	1.265	0.085
8	H	0.813	1.982	-0.550
9	H	0.387	1.644	1.114
10	C	0.973	-0.088	0.005
11	N	0.396	-1.224	-0.087
12	C	1.065	-1.307	-0.116
13	H	-1.350	-2.174	0.493
14	H	-1.349	-1.564	-1.148
15	C	2.483	-0.054	0.044
16	H	2.883	0.489	-0.823
17	H	2.840	0.473	0.939
18	H	2.880	-1.071	0.043

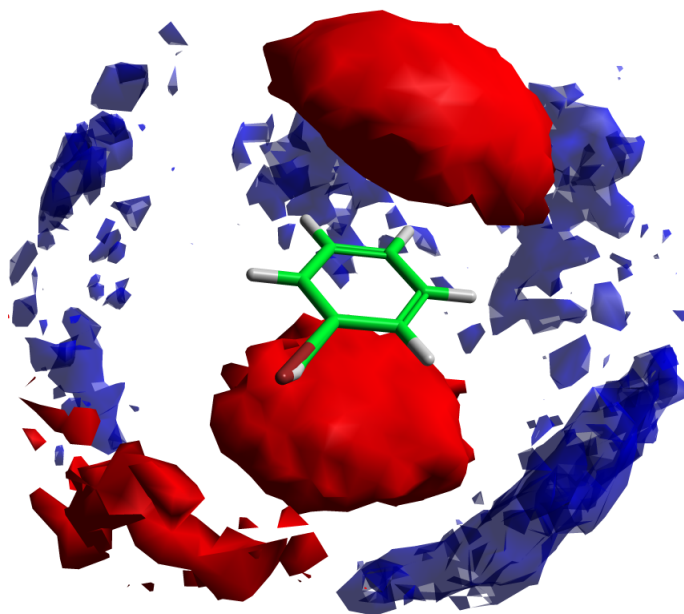


Figure S1. Coordination around the bromide **1d**, showing cation interactions (red, cut-off 0.005) above and below the aromatic ring, and anion interactions (blue, cut-off 0.005) about the equator.

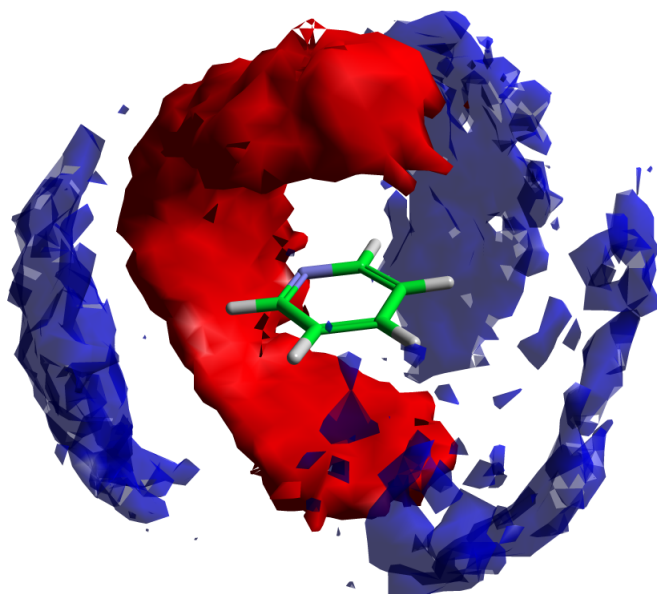


Figure S2. Coordination about the pyridine **2**, showing cation interactions (red, cut-off 0.005) both above and below the aromatic ring and with the nitrogen centre, and anion interactions (blue, cut-off 0.005) in three distinct bands about the equator.

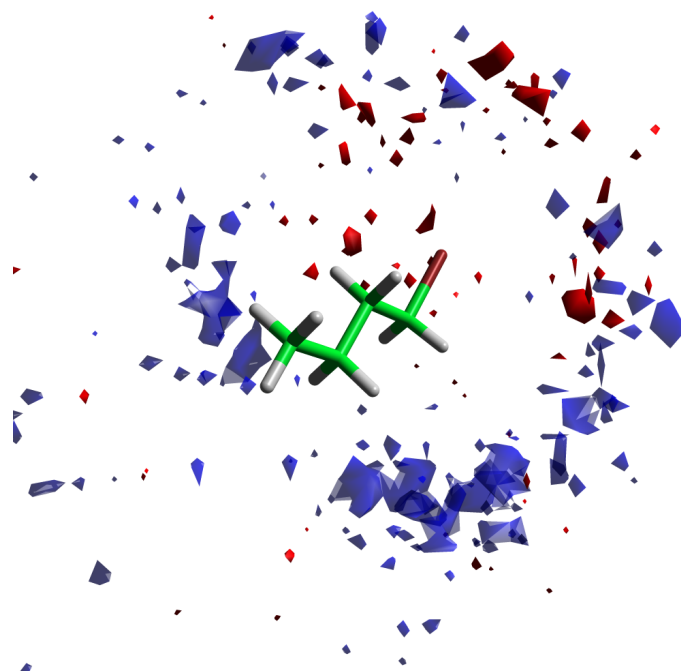


Figure S3. Organisation profile of the ionic liquid around *n*-bromobutane **4** with showing interaction with the cation (red, cut-off 0.008) and the anion (blue, cut-off 0.008). No distinct regions of localisation can be seen.

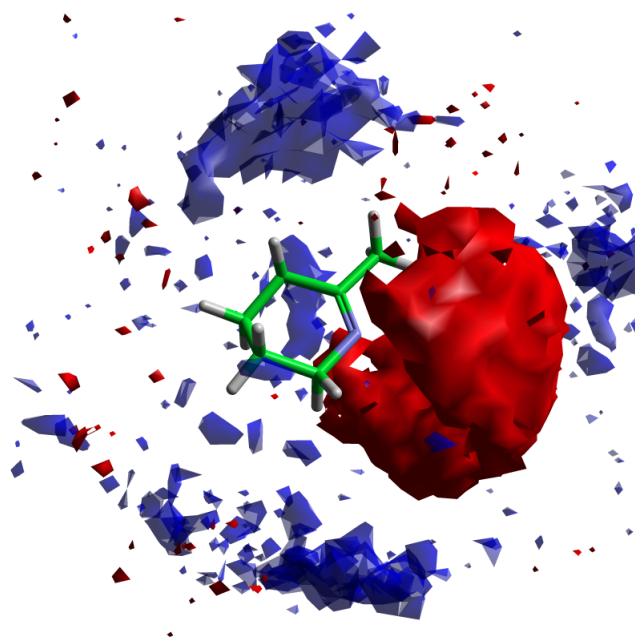


Figure S4. Coordination around the imine **7** showing cation interactions (red, cut-off 0.008) with the nitrogen centre. No distinct anion interactions with the imine **7** are discernible, though localised regions can be seen (blue, cut-off 0.008).

1. Y. Chan, X. Li, C. Zhu, X. Liu, Y. Zhang and H. Leung, *J. Org. Chem.*, 1990, **55**, 5497.
2. M. J. Panigot, M. J. Robarge and R. W. Curley, *AAPS PharmSci*, 2001, **3**, 26.
3. E. P. Anderson, J. V. Crawford and M. L. Sherrill, *J. Am. Chem. Soc.*, 1946, **68**, 1294.
4. C.-H. Lee, J.-S. Lee, H.-K. Na, D.-W. Yoon, H. Miyaji and W.-S. Cho, *J. Org. Chem.*, 2005, **70**, 2067.
5. G. W. T. M. J. Frisch, H. B. Schlegel, G. E. Scuseria, J. R. C. M. A. Robb, J. A. Montgomery, Jr., T. Vreven, J. C. B. K. N. Kudin, J. M. Millam, S. S. Iyengar, J. Tomasi, B. M. V. Barone, M. Cossi, G. Scalmani, N. Rega, H. N. G. A. Petersson, M. Hada, M. Ehara, K. Toyota, J. H. R. Fukuda, M. Ishida, T. Nakajima, Y. Honda, O. Kitao, M. K. H. Nakai, X. Li, J. E. Knox, H. P. Hratchian, J. B. Cross, J. J. C. Adamo, R. Gomperts, R. E. Stratmann, O. Yazyev, R. C. A. J. Austin, C. Pomelli, J. W. Ochterski, P. Y. Ayala, G. A. V. K. Morokuma, P. Salvador, J. J. Dannenberg, S. D. V. G. Zakrzewski, A. D. Daniels, M. C. Strain, D. K. M. O. Farkas, A. D. Rabuck, K. Raghavachari, J. V. O. J. B. Foresman, Q. Cui, A. G. Baboul, S. Clifford, B. B. S. J. Cioslowski, G. Liu, A. Liashenko, P. Piskorz, R. L. M. I. Komaromi, D. J. Fox, T. Keith, M. A. Al-Laham, A. N. C. Y. Peng, M. Challacombe, P. M. W. Gill, and W. C. B. Johnson, M. W. Wong, C. Gonzalez, and J. A. Pople, Gaussian, Inc., Pittsburgh PA, 2003.
6. M. W. Schmidt, K. K. Baldridge, J. A. Boatz, S. T. Elbert, M. S. Gordon, J. H. Jensen, S. Koseki, N. Matsunaga, K. A. Nguyen, S. J. Su, W. L. Windus, M. Dupuis and J. A. Montgomery, *J. Comput. Chem.*, 1993, **14**, 1347-1363.
7. W. Smith, M. Leslie and T. R. Forester, *The DL_POLY_2 Reference Manual*, Warrington, CCLRC, Daresbury Laboratory, 2003.
8. T. G. A. Youngs, *J. Comput. Chem.*, 2009, **31**, 639.
9. J. N. Canongia Lopes, J. Deschamps and A. A. H. Pádua, *J. Phys. Chem. B*, 2004, **108**, 2038-2047.
10. W. L. Jorgensen, D. S. Maxwell and J. Tirado-Rives, *J. Am. Chem. Soc.*, 1996, **118**, 11225-11236.
11. W. L. Jorgensen and N. A. McDonald, *Theochem.*, 1998, **424**, 145-155.
12. R. C. Rizzo and W. L. Jorgensen, *J. Am. Chem. Soc.*, 1999, **121**, 4827-4836.
13. C. G. Hanke, S. L. Price and R. M. Lynden-Bell, *Mol. Phys.*, 2001, **99**, 801-809.
14. E. K. Watkins and W. L. Jorgensen, *J. Phys. Chem. A*, 2001, **105**, 4118-4125.